Controlled-chemical etching of the cladding in optical fibers for the design of analytical sensors

Dorian Meunier[1], Jérôme Schruyers[2], Rachel Gonzales Palla[1], Carlos Mendoza[1], Cédric Calberg[3], Benoît Heinrichs[3], Sophie Pirard[1], Julien G. Mahy[3,4]*

[1] Haute Ecole Libre Mosanne (HELMo), Centre de Recherches des Instituts Groupés de HELMo (CRIG), Liège, Belgium

[2] B-SεNS, Boulevard Dolez 31, 7000 Mons, Belgium

[3] Department of Chemical Engineering – Nanomaterials, Catalysis & Electrochemistry, University of Liège, B6a, Quartier Agora, Allée du six Août 11, 4000 Liège, Belgium

[4] Institut National de la Recherche Scientifique (INRS), Centre-Eau Terre Environnement, Université du Québec, 490, Rue de la Couronne, Québec (QC), G1K 9A9, Canada

*Corresponding author: Julien G. Mahy; email: julien.mahy@uliege.be ; address: Allée du Six Août 11, 4000 Liège, Belgium

Abstract

An optimized chemical method is developed for etching the cladding of an optical fiber without degrading its core. The goal is to obtain a smooth core surface that will be used further for sensor development. This technique consists of attacking the cladding with a buffer solution made of fluorinated salts. Three different concentrations in the buffer are used: 20%, 40%, and 60%. The bare core could then be used for sensing application thanks to interaction with the light signal.

By following the evolution of the fiber diameter with the etching time, two different kinetics are observed for each concentration. These two parts of the curve correspond to the attack of the cladding and the core, and the transition point allows to find the time when the cladding is removed. With increased buffer concentration, this etching time is decreased. Concerning the evolution of a light signal transmitted throughout the fiber during the attack, three zones are observed on the transmitted signal: (i) a small linear decrease at the beginning of the attack (degradation of the cladding), (ii) a high drop in transmission (cladding is removed), and (iii) again a small linear decrease of the transmission (progressive degradation of the core). The more the buffer concentration is high, the higher is the transmitted signal loss.

Finally, an optimized chemical condition is determined to obtain a good compromise between the time of etching and the resulting signal loss in transmission while limiting the chemical risks associated to the use of fluorinated salts.

Keywords: Etching, HF, Cladding, Optical Fiber, Surface Treatment, Chemical Attack

1. Introduction

Fiber-optic Evanescent Wave Spectroscopy Sensors (FEWS) are increasingly being developed and have emerged to be applied as biochemical, biomedical, and environmental sensors [1,2]. Some advantages of this kind of sensors include small size, immunity to electromagnetic and radio frequency interference, remote sensing, multiplicity of information from a large number of sensors into a single fiber, and in certain cases, low cost. An alternative design for a fiber sensor involves the replacement of the different sections of the optical fiber with nanoparticles or coatings [3–6]. Indeed, typically an optical fiber is made of a pure silica core with a high refractive index covered by a cladding with lower refractive index [7,8]. The fiber can then be covered by a polymer for mechanical and chemical protection. To modify the optical fiber in order to use it as a sensor, the transmitted signal must interact with the external medium, which can be possible only if the cladding is removed [9]. This operation is called the etching [10], and it is a very sensitive step to avoid degrading the core of the fiber which can result in signal losses [11,12]. So, a main challenge is the chemical etching of the cladding part, generally made of doped silica, without damaging the core.

To etch the cladding of a fiber, HF is generally used because of its high reactivity towards silica [9,10,13,14], etching cream can also be used [15]. Reactions of HF with silica are represented as [1,16]:

$SiO_2 + 4HF \rightarrow SiF_4 + 2H_2O$ (1)

$SiO_2 + 6HF \rightarrow H_2SiF_6 + 2H_2O$ (2)

Etching rate is increased when HF concentration is maximized [2]. However, HF concentration and its diffusion through the silica lattice are usually ignored when preparing chemical etching. In previous

works [11,12], high HF concentrations have led to heterogeneous surfaces and high optical losses have been attributed to the formation of surface corrugations and roughness during the chemical etching. Moreover, the use of HF is very dangerous for the operator [15]. In order to avoid this effect, buffer solutions with a low concentration of HF can be prepared controlling the surface conditions of the core, reducing also the hazard of the process [11,12,17,18]. These compounds have still important risks associated to their use as acute toxicity, skin corrosion/irritation, serious eye damage/eye irritation, respiratory or skin sensitization and it is necessary to wear protective gloves/protective clothing/eye protection/ face protection when working with them [19]. Nevertheless, it is less aggressive to work with fluorinated slats than HF [20]. The control of the etching time is an important parameter: it must be long enough to remove the cladding layer, but short enough to avoid a degradation of the silica core of the fiber.

In this work, it is reported a new controlled method to remove the cladding part of an optical fiber using 20, 40 and 60% w:v buffer solution (pH=3.5) of fluorinated salts, obtaining a homogeneous surface of the core through a safer process. The etching time will be determined for each etching solution and the evolution of a lighting signal during the etching process will be also assessed. An optimal buffer concentration and etching time will be given, taking into account the quality of the fiber core, the time of etching and the risks for the operator. SEM images of the fibers will show the different surface aspects throughout the process.

2. Experimental

2.1. Optical fiber materials

Ultraviolet, non-solarizing optical fibers from Thorlabs (FG105ACA) were employed. These fibers, whose specifications are represented in Table 1, present a broad spectral range (180 – 1200 nm) and high laser damage resistance, ideal for a variety of applications, such as spectroscopy, UV photolithography, laser delivery, and medical diagnostics, specifically between 190 – 325 nm.

Table 1: Specifications of the Thorlabs FG105ACA Fiber.

Specifications

Core Diameter	105 ± 2.1 µm
Core Material	Silica SiO_2
Core Refractive Index	1.457405
Cladding Diameter	125 ± 1 µm
Cladding Material	F-Doped Silica
Cladding Refractive Index	1.43944
Coating Diameter	250 ± 10 µm
Coating Material	Acrylate
Operating Wavelength	180 – 1200 nm
Operating Temperature	-40 to 85 ºC

80

81 2.2. Etching protocol and microscope analysis

82 As mentioned in the introduction, to control the homogeneity of the chemical etching, a buffer
83 solution of ammonium fluoride (NH_4F) and ammonium hydrogen difluoride (NH_4HF_2) (Sigma-Aldrich)
84 was prepared. A certain amount of these salts were added to 20 mL of water to obtain 3 different salt
85 concentrations: 20, 40 and 60% w:v solutions. To have a pH equal to 3.5, these salts were in a ratio
86 3.72:1 (w:w, NH_4F:NH_4HF_2). Before the etching, the acrylate coating around the fiber was removed
87 with the help of a stripper after immersing the fiber parts in dichloromethane in order to soften the
88 polymer facilitating its mechanical removal with the stripper. A fiber was then immersed in 500 µL of
89 one of this buffer solution inside a single-slot 3D-printed support (around 4 cm to etch) in order to
90 reduce hazard. For each concentration, different etching times were performed in order to evaluate
91 when the cladding layer was removed. In these cases, a multiple-slot 3D-printed support was used to
92 etch several fibers in parallel with the same concentration, by removing those fibers after specific
93 times. Etched optical fibers were taken out, abundantly rinsed with distilled water to completely stop
94 the reaction, and then they were observed with optical microscopy to determine their diameters. The
95 evolution of the fiber diameter with time can be followed for each etching solution, each point of
96 theses curves was made 4 times to assess the reproducibility.

The surface aspect of the fibers was also observed with field emission gun scanning electron microscopy (FEG-SEM). The optical fibers to observe were attached on a glass slide. Then these slides were analyzed by the Sigma 300 FEG-SEM from ZEISS at a magnification of 600X.

2.3. Set-up for optical measurements

In order to measurement the influence of the chemical etching of the optical fiber on a light signal transmitted throughout the fibers, the following set-up was made. The optical fibers were connected to a stabilized deuterium UV light source (SLS204, Thorlabs) which provided a broad emission spectrum (200-700 nm) with a strong continuous spectrum at short UV wavelengths (200-400 nm). Figure 1 shows the emission spectrum of the light source.

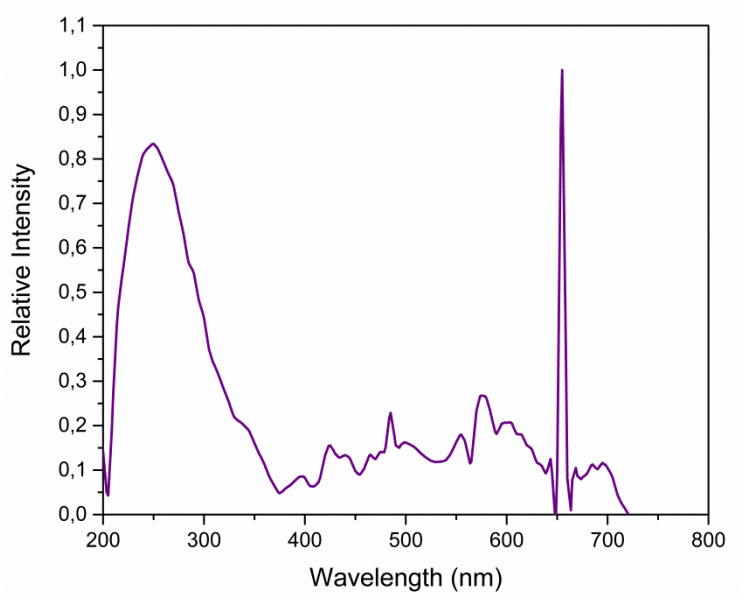

Figure 1: Emission spectrum of the UV light source

The other side of the fiber was connected to a CCD Spectrometer (Thorlabs, CCS200/M) that continuously recorded the spectra between 200 and 1000 nm (Figure 2a). To achieve this configuration, 2 cm of the acrylate coating from both sides were removed, as well as 4 cm of the center to perform the chemical etching in a polypropylene 3D-printed support. The etching was made with the three buffer concentrations as detailed in the previous section. The acrylate coating was removed with the help of a stripper after immersing the fiber parts in dichloromethane. The final structure of the optical fiber, where the etching took place, contained only the core part, as shown in Figure 2b.

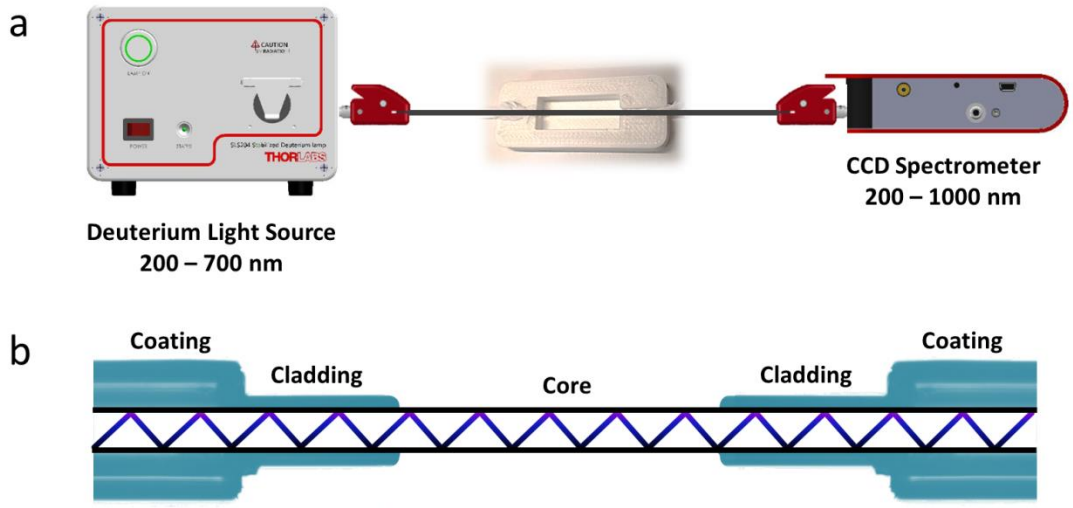

Figure 2: (a) Experimental setup and (b) Schematic representation of the core / cladding / coating structure

3. Results and Discussion

3.1. Study of the fiber diameter evolution with the etching time

Figure 3 represents the evolution of the optical fiber diameter with the etching time for the three different buffer concentrations. For each concentration, it is observed that the diameter decreases with etching time as expected, but two behaviors are noticed. Indeed, there is a change in the slope of the etching curve, and for each concentration, after a specific time, the etching is slower. The first part of the curve (4 first points) corresponds to the etching of the cladding layer, then, the second part (4 last points) corresponds to the etching of the core of the fiber. The cladding is etched faster than the core in each case. Indeed, the cladding is made of silica doped with fluorine [18] with is more easily degraded by the buffer solution than pure silica which composed the core of the fiber [18]. In fact, the cladding layer is made of F-doped silica which contains defects due to the presence of fluorine ions [21]. These defects allow a faster degradation of the silica network by the reaction 1 and 2. Moreover, fluoride ions that are involved in the HF/F- equilibrium are already present in the silica, increasing the degradation rate of the network [22]. Table 2 denotes the curve equations for each layer with the three concentrations, the change in the slope is mathematically observed. For each concentration, a linear regression is fitted to the two sets of points, giving the two curve equations for the

cladding and the core etchings as denoted in Table 2 (six curve equations in total for the six sets of points).

In Table 2, the ratio of the slope is also calculated for each concentration. This ratio is around 2.5 for the three concentrations, meaning that ratio of the kinetic of etching between the cladding and the core is the same for the three concentrations.

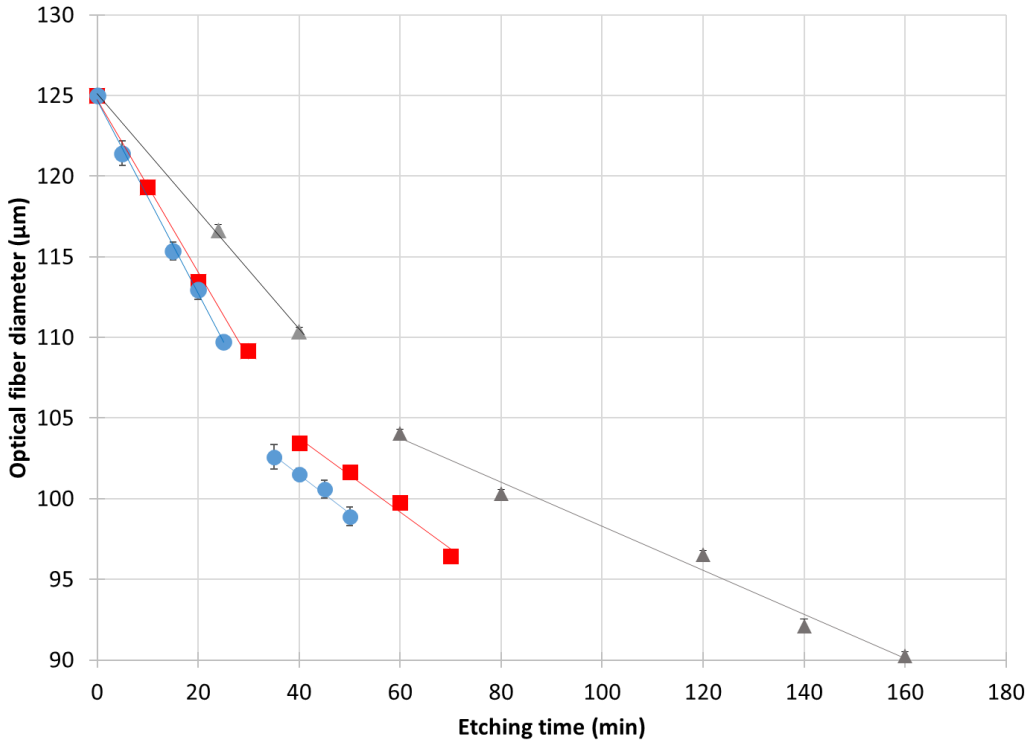

Figure 3: Diameter of the fiber in function of the etching time for (▲) 20%, (■) 40% and (●) 60% buffer. Each point is made 4 times, the error bars are really small due to the very low variability on the measurements. For some points, the error bars are even smaller than the symbol used for the series.

Table 2: Equations of the etching curves of Figure 3 and the corresponding R^2.

Buffer solution	Cladding etching		Core etching		Slope ratio cladding/core
	Equation	R^2	Equation	R^2	
20%	y = -0.3643x + 125.11	0.9989	y = -0.1363x + 111.92	0.9835	2.7

40%	y = -0.5336x + 124.73	0.9954	y = -0.2298x + 112.95	0.9755	2.3
60%	y = -0.5999x + 124.69	0.9976	y = -0.2398x + 111.09	0.9807	2.5

When the buffer solution concentration increases, the etching is faster. Indeed, the slope increases with the concentration. The point where the slope changes can be considered as the time when the cladding layer is totally removed, called T_C. This time is equal to 58, 39, and 37 min for the 20%, 40%, and 60% buffer solution respectively. Depending on the concentration, the optimal etching time (T_E) must be chosen a bit bigger than T_C to be sure that the attack is completed, and that all the cladding layer is removed.

Figure 4 illustrates the surface aspect of the fiber after different etching times (30, 33, 36 39 and 42 min) for the 60% buffer solution. The homogeneous attack is clearly observed, after 30 min (Figure 4a), the cladding layer is ~~a~~ partially degraded and a rough surface is noticed. With the etching time increasing, the surface goes smoother. Around the time T_C determined on the Figure 3 for 60% buffer solution (37 min), the surface is almost smooth (Figures 4c and d) and after some more minutes, the surface is finally perfectly smooth meaning that all the cladding is removed homogeneously.

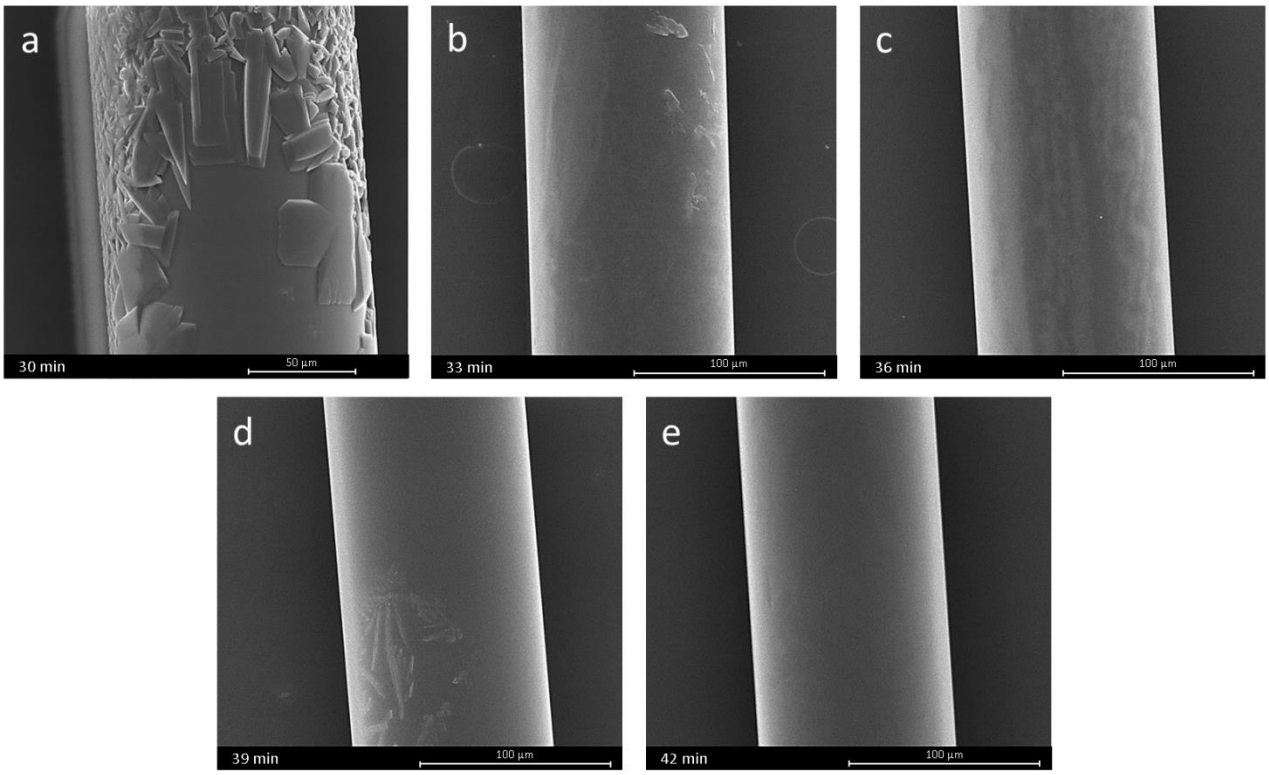

Figure 4: SEM images of the optical fibers at (a) 30, (b) 33, (c) 36, (d) 39, and (e) 42 min of etching time in the 60% buffer etching solution at a magnification of 600 X.

3.2. Study of the signal transmission with the etching time

Light transmission of the optical fiber was continuously registered during the chemical etching using the CDD spectrophotometer, the three concentrations were evaluated. Figure 5 shows the different spectra obtained as a function of the etching time for the three buffer solutions.

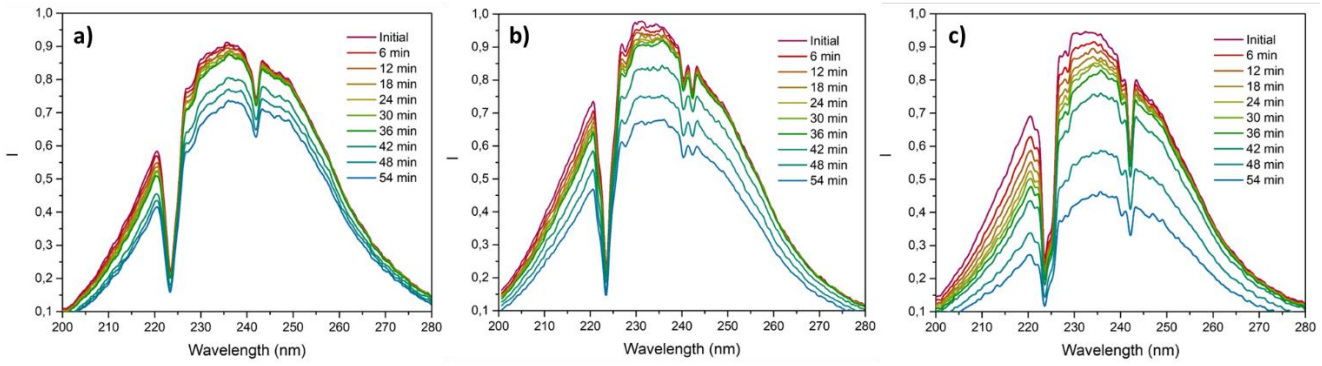

Figure 5: Evolution of the transmittance through the optical fiber in the range 200-280 nm as a function of the etching time (total time of 54 min) for an optical fiber treated in the (a) 20%, (b) 40%, and (c) 60% buffer solution.

The signal of the obtained spectra decreases as a function of the time. It indicates that the cladding is etched from the beginning of the process. These peak areas were monitored during the etching time for the three different concentrations. Indeed, Figure 6 presents the obtained relative intensities (I/I_0) in function of the etching time for the three concentrations. The first observation from Figure 6 is the presence of two plateaus and a transition region in the three cases. The transition region appears faster with the increase in the concentration and the loss in signal intensity increases also with the concentration. The modifications of the signal intensity and the influence of the buffer concentrations are explained in the following paragraph.

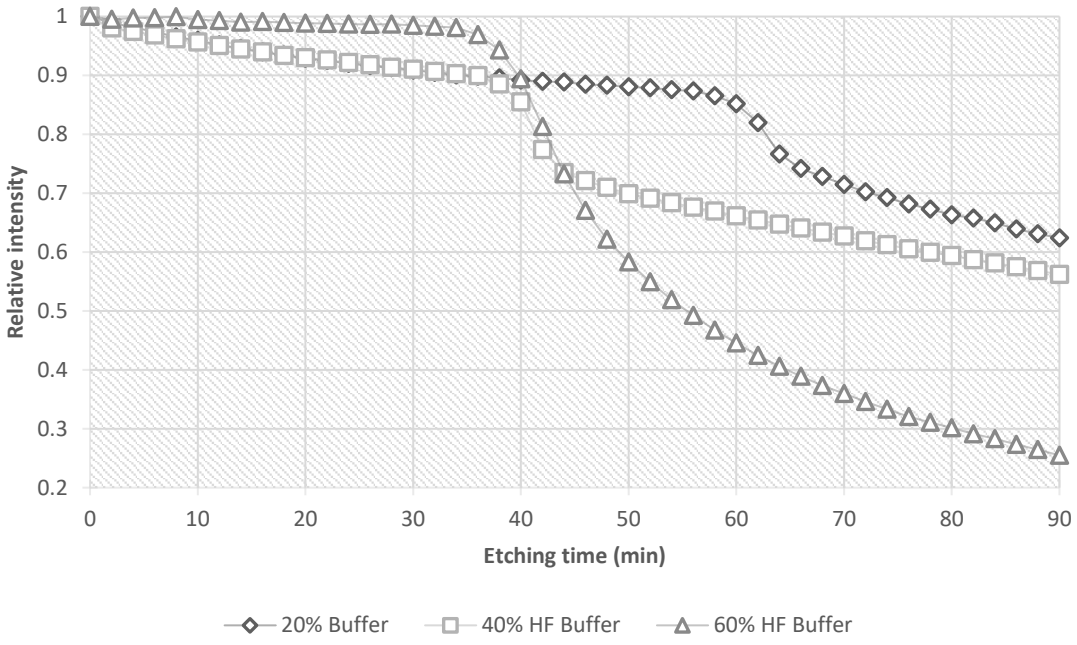

Figure 6: Relative intensity of the signal in function of the etching time for the (◊) 20%, (□) 40%, and (Δ) 60% buffer solutions.

Regarding the Snell-Descartes law [23,24], the limit angle to have a total reflection of the light at an interface of two different materials having their own refractive index (Figure 7) can be described as (equation 3):

$$\propto = \mathbf{arcsin}\left(\frac{n_2}{n_1}\right) \quad (3)$$

Where n_1 and n_2 are the refractive index of the core and the cladding, respectively.

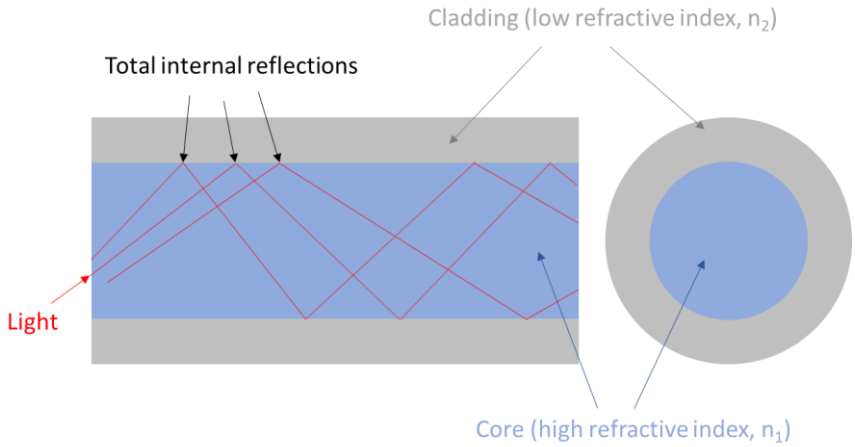

Figure 7: Reflection of the light through an optical fiber [10].

In other words, the light is reflected through the whole fiber due to the difference of the refractive indexes of the core (n_1) and the cladding (n_2). The removal of the cladding leads then to 3 situations which correspond to the three parts of the curves observed on Figure 6.

The first situation, which consists of the first plateau observed in Figure 6, is the removal of the cladding without reaching the core. In this situation, the refractive index of the cladding slightly changes, leading to a faint decrease of the signal transmission.

The second phase is the transition phase, where the light transmission falls (Figure 6). This is due to the reach of the core. Throughout the fall, cladding is removed, and the external material becomes the aqueous medium, having a refractive index of 1.2. Regarding the Snell-Descartes law (equation 3), the limit angle decreases and the rays, which had satisfying incidence angles, are now ejected out of the fiber, leading to signal losses.

Once the cladding is completely removed (second plateau on Figure 6), the fall slows down, but the signal transmission continues to decrease. This third situation is due to formation of inhomogeneities (pores) in the core as the attack continues. Indeed, the study by Zhong et al. [11,12] has concluded that the deeper and larger the pores, the more affected the signal is. This is also why buffered solutions are used to avoid signal losses, to be the most homogeneous as possible with the attack.

Concerning the influence of the buffer concentration on the signal, according to Zhong et al. [11,12], the reactive species are HF_2^- and H_2F_2 and their concentrations increase with a more concentrated buffer, increasing the etching rate. This is what is observed here, indeed, for the 20%, 40% and 60% buffers, the transition region is reached after 60, 39 and 36 minutes, respectively. In the 20% and 40% buffer, the core is reached at 64 and 44 minutes, respectively. For the 60% buffer, it is more difficult to determine probably due to a fast degradation of the core.

So, by following the signal transmission evolution with etching time, it can be also deduced the time where the cladding layer is removed (T_C) as did before on Figure 3. The T_C values are 60, 39, and 36 min for 20%, 40%, and 60% respectively. These values are really close to the values obtained with Figure 3, confirming that these are the etching times to remove the cladding. The small differences can be due to the use of different optical fibers which can have cladding with not exactly the same thickness from one fiber to another (Table 1).

From the diameter measurements (Figure 3) and the signal transmission evolution (Figure 6), it results that the 40% buffer solution is the most suitable solution for the etching of optical fiber, combining a fast removing of the cladding (45 min – Figure 3, to ensure a complete removal of the cladding), a lower dangerous HF molecules contents, and a low loss of signal transmission (Figure 6).

4. Conclusions

In this work, a method for etching the cladding layer of an optical fiber is developed in order to find the optimized conditions to remove this layer without degrading the core of the fiber. This method consists of a controlled chemical attack of the cladding with a buffer solution made of ammonium fluoride (NH_4F) and ammonium hydrogen difluoride (NH_4HF_2) salts. Three different concentrations in the buffer are used: 20%, 40%, and 60%. The influence of this treatment is studied on the evolution of the fiber diameter with the etching time and on the transmission of a UV light signal. The bare core can then be used for sensing application thanks to interaction with the light.

Results have shown that the fiber diameter decreases with the etching time with two different kinetics depending if the cladding or the core is attacked. The transition in the etching kinetics allows to find the etching time to remove the cladding. When the concentration of the buffer is increased, the kinetic of etching is increased. By following the transmission of a light signal in the fiber during the etching, the etching time to remove the cladding can be also determined to obtain the same time value when following the diameter. Indeed, the signal transmission is divided into three zones: (i) a small decrease in the transmission when the cladding is partially attack, (ii) a high drop in transmission when the cladding is removed, and (iii) a small decrease in the signal when the core of the fiber is bare.

Finally, these characterizations allowed to determine the optimized chemical conditions to etch optical fibers which is to use the 40% buffer solution for 45 min to remove the cladding. This condition gives a good compromised between the time of etching and the resulting signal loss in transmission. Moreover, the 40% concentration limits the chemical risks associated to the use of fluorinated salts. Once the optical fiber is properly etched, it opens the way for the development of sensor thanks to the interaction between the light signal and the external medium on this etched zone.

Acknowledgements

The research was funded through the MOUV (UV Sensor for Continuous Monitoring of Organic Pollutants in Water) project, a Win2Wal grant, financed by the French Community of Belgium.

Julien G. Mahy thanks the F.R.S.-FNRS for his Postdoctoral Researcher position. J.G.M. is also grateful to the Rotary for a District 2160 grant, to the University of Liège and the FNRS for financial support for a postdoctoral stay in INRS Centre Eau, Terre, Environnement in Québec, Canada.

Data Availability Statement

The raw/processed data required to reproduce these findings cannot be shared at this time as these data are part of an ongoing study.

Conflict of interest

The authors declare that there is no conflict of interest concerning this work.

Ethical Approval

The authors declare that they have no known competing financial interests or personal relationships that could have appeared to influence the work reported in this paper.

Authors Contributions

Dorian Meunier: Conceptualization, Methodology, Investigation, Formal analysis, Writing – review & editing. Jérôme Schruyers: Conceptualization, Methodology, Investigation, Formal analysis Writing – review & editing. Rachel Palla Gonzalez: Conceptualization, Investigation, Formal analysis, Writing – review & editing. Carlos Mendoza: Conceptualization, Methodology, Investigation, Formal analysis Writing – review & editing. Cédric Calberg: Investigation, Formal analysis, Writing – review & editing. Benoît Heinrichs: Conceptualization, Methodology, Formal analysis, Writing – review & editing, Financial support, Project administration. Sophie Pirard: Conceptualization, Methodology, Formal analysis, Writing – review & editing, Financial support, Project administration. Julien G. Mahy: Investigation, Formal analysis, Supervision, Writing – original draft, Writing – review & editing.

References

[1] L.F. Rickelt, L.D.M. Ottosen, M. Kühl, Etching of multimode optical glass fibers: A new method for shaping the measuring tip and immobilization of indicator dyes in recessed fiber-optic microprobes, Sens Actuators B Chem. 211 (2015) 462–468. https://doi.org/10.1016/j.snb.2015.01.091.

[2] M.H. Younus, O.F. Ameen, N. Redzuan, N. Ahmad, R.K. Raja Ibrahim, Fabrication and characterization of multimode optical fiber sensor for chemical temperature monitoring using optical time domain reflectometer, Karbala International Journal of Modern Science. 4 (2018) 119–125. https://doi.org/10.1016/j.kijoms.2017.12.002.

[3] Y. Shao, S. Xu, X. Zheng, Y. Wang, W. Xu, Optical fiber LSPR biosensor prepared by gold nanoparticle assembly on polyelectrolyte multilayer, Sensors. 10 (2010) 3585–3596. https://doi.org/10.3390/s100403585.

[4] H.K. Bal, Z. Brodzeli, N.M. Dragomir, S.F. Collins, F. Sidiroglou, Uniformly thinned optical fibers produced via HF etching with spectral and microscopic verification, Appl Opt. 51 (2012) 2282–2287.

[5] Z. Samavati, A. Samavati, A.F. Ismail, N. Yahya, M.A. Rahman, M.H.D. Othman, Effect of acetone/methanol ratio as a hybrid solvent on fabrication of polymethylmethacrylate optical fiber sensor, Opt Laser Technol. 123 (2020). https://doi.org/10.1016/j.optlastec.2019.105896.

[6] B. Patiño-Jurado, Y. Cardona-Maya, M. Jaramillo-Grajales, Y.J. Montagut-Ferizzola, J.F. Botero-Cadavid, A label-free biosensor based on E-SMS optical fiber structure for anti BSA detection, Optical Fiber Technology. 74 (2022). https://doi.org/10.1016/j.yofte.2022.103116.

[7] P. Guenot, Material Aspects of Standard Transmission Optical Fibers Different Types of Fibers, MRS Bull. (2003) 360–364.

[8] V. Degiorgio, I. Cristiani, Optical Fibers, in: F. Bassani, G.L. Liedl, P. Wyder (Eds.), Encyclopedia of Condensed Matter Physics, Elsevier, Oxford, 2005: pp. 152–158. https://doi.org/https://doi.org/10.1016/B0-12-369401-9/01148-7.

[9] M. Chauhan, V.K. Singh, Tapered MMF sensor fabrication using SnO2-NPs for alcohol sensing application, Optical Fiber Technology. 75 (2023). https://doi.org/10.1016/j.yofte.2022.103167.

[10] M.A. Riza, Y.I. Go, R.R.J. Maier, S.W. Harun, S.B.A. Anas, Enhanced fiber mounting and etching technique for optimized optical power transmission at critical cladding thickness for fiber-sensing application, Laser Phys. 31 (2021). https://doi.org/10.1088/1555-6611/ac3014.

[11] N. Zhong, Q. Liao, X. Zhu, Y. Wang, R. Chen, High-quality fiber fabrication in buffered hydrofluoric acid solution with ultrasonic agitation, Appl Opt. 52 (2013) 1432–1440.

[12] N. Zhong, X. Zhu, Q. Liao, Y. Wang, R. Chen, Y. Sun, Effects of surface roughness on optical properties and sensitivity of fiber-optic evanescent wave sensors, Appl Opt. 52 (2013) 3937–3945. https://doi.org/10.1364/AO.52.003937.

[13] M.A. Riza, Y.I. Go, R.R.J. Maier, Dynamics rate of fiber chemical etching: New partial removal of cladding technique for humidity sensing application, Laser Phys. 30 (2020). https://doi.org/10.1088/1555-6611/abbe83.

[14] P. Zaca-Morán, J.M. Cuvas-Limón, J.P. Padilla-Martínez, C. Amaxal-Cuatetl, L.C. Gómez-Pavón, R. Zaca-Morán, J.G. Ortega-Mendoza, Experimental study of saturable and reverse saturable absorption of Zn nanoparticles photodeposited onto etched optical fibers, Opt Commun. (2022) 129032. https://doi.org/10.1016/j.optcom.2022.129032.

[15] H.W. Ding, J.D. Shi, T.W. Lim, Y.C. Tan, W.J. Lai, Economical Solution for Cladding Etched Optical Fibers, in: 2019 18th International Conference on Optical Communications and Networks (ICOCN), 2019: p. 8934123.

[16] R.M. Chyad, M. Zubir Mat Jafri, K. ulazizi Ibrahim, Fabrication nano fiber optic by chemical etching for sensing application The 5 th International Scientific Conference for Fabrication nano fiber optic by chemical Etching for sensing application 995, Nanotechnology and Advanced Materials and Their Applications ICNAMA. 3 (2015) 3.

[17] A. Witvrouw, B. du Bojsab, D. Moora, A. Verbista, C. van Hoof', H. Bendera, K. Baerta, A comparison between wet HF etching and vapor HF etching for sacrificial oxide removal, Micromachining and Microfabrication Process Technology VI. 4174 (2000) 130–141. http://proceedings.spiedigitallibrary.org/.

[18] D.J. Markos, B.L. Ipson, K.H. Smith, S.M. Schultz, R.H. Selfridge, T.D. Monte, R.B. Dyott, G. Miller, Controlled core removal from a D-shaped optical fiber, Appl Opt. 42 (2003) 7121–7125.

[19] Sigma-Aldrich, Ammonium hydrogen difluoride, (2023). Ammonium hydrogen difluoride (accessed March 24, 2023).

[20] J.S. Judge, A Study of the Dissolution of SiO in Acidic Fluoride Solutions, J Electrochem Soc. 118 (1971) 1772–1775.

[21] S. Todoroji, S. Sakaguchi, Effect of F-Doping on Optical and Thermal Properties of Soda Magnesium Silicate Glasses for Utralow-Loss Fibers, Jpn J Appl Phys. 35 (1996) 5374–5378.

[22] H. Kikuyama, M. Waki, M. Miyashita, T. Yabune, N. Miki, A Study of the Dissociation State and the SiO2 Etching Reaction for HF Solutions of Extremely Low Concentration, J Electrochem Soc. 141 (1994) 366–374.

[23] A. Pisano, Physics for Anesthesiologists and Intensivists From Daily Life to Clinical Practice Second Edition, Second edition, Springer Nature, 2021.

[24] J. Keirsse, C. Boussard-Plédel, O. Loréal, O. Sire, B. Bureau, P. Leroyer, B. Turlin, J. Lucas, IR optical fiber sensor for biomedical applications, in: Vib Spectrosc, Elsevier, 2003: pp. 23–32. https://doi.org/10.1016/S0924-2031(03)00044-4.